Renewable Energy 77 (2015) 442–446

Contents lists available at ScienceDirect

Renewable Energy

journal homepage: www.elsevier.com/locate/renene

Review

Numerical simulations of multilevel impurity photovoltaic effect in the sulfur doped crystalline silicon

E.T. Hu [a], G.Q. Yue [a], R.J. Zhang [a], Y.X. Zheng [a], L.Y. Chen [a], S.Y. Wang [a, b, *]

[a] Shanghai Ultra-Precision Optical Manufacturing Engineering Center and Department of Optical Science and Engineering, Fudan University, Shanghai 200433, China
[b] Key Laboratory for Information Science of Electromagnetic Waves (MoE), Shanghai 200433, China

ARTICLE INFO

Article history:
Received 1 May 2014
Accepted 19 December 2014
Available online 5 January 2015

Keywords:
Silicon solar cell
Multilevel IPV effect
SCAPS simulator

ABSTRACT

The multilevel impurity photovoltaic effect (IPV) of the sulfur doped crystalline silicon (c-Si) is studied by using the SCAPS program. The effects of impurity concentration (N_t) of two and four defect levels on the performance of sulfur doping c-Si solar cell are investigated, respectively. Then, the quantum efficiencies (QE) of different cases (without impurity, two and four defect levels) are considered. The results show that after the doping of sulfur, the infrared response of the c-Si solar cell is enhanced. Moreover, the infrared response wavelength range of the case considering two defect levels may be wider than that of four defect levels. In order to get the highest photovoltaic conversion efficiency (PCE), the number and the type of defect levels should be controlled. In the end, with four defect levels considered, the thickness and background doping concentration (N_D for the n-type layer and N_a for the p-type layer) of each layer of the n^+–p–p^+ structure are optimized. Our results suggest that higher PCE could be achieved than that without impurity by choosing a suitable doping concentration. The efficiency of 25.32% attained in the four-defect case improved the PCE by 2% more than the value of 23.22% without sulfur doping.

1. Introduction

For the single band solar cells, the most important power-loss mechanism is the inability to absorb photons with energies less than the band gap. In order to overcome this problem, the impurity photovoltaic (IPV) effect is introduced as a potential approach that has attracted much attention in recent years [1–5]. The concept of the IPV effect is to introduce impurity levels into the band gap. The impurity levels act as stepping stones when electrons are excited from the valence band (VB) to the conduction band (CB). Thus even the sub-band photons can be absorbed. Therefore, the short circuit current density (J_{sc}) and the long wavelength spectral response will be enhanced. However, the defect levels also play a role as recombination centers, which will enhance the recombination of free carriers and decrease the open circuit voltage (V_{oc}) of solar cells. In order to suppress the opposite effect and get a photovoltaic conversion efficiency (PCE) improvement through IPV, a lot of efforts have been done.

By using a modified Shockley–Read–Hall (SRH) recombination model and the superposition approach, a 1–2% efficiency improvement was achieved through indium doping in a silicon solar cell in 1994 by Keevers et al. [1]. However, in 1999, Schmeit et al. [2] found that when the indium doped silicon solar cell was used in the p-n structure, the efficiency could not be improved because of the rapid decreasing of voltage which was not considered by Keevers due to the superposition approach used by them. In order to overcome the shortcoming, they used the p-n-n^+ structure and a 0.7–1% efficiency improvement was obtained. The impurity of copper [6], sulfur [7] and thallium [8] or the wide band gap host materials such as GaAs [6], β-SiC [4] were studied as well.

The infrared absorbance was reported to be enhanced by incorporation of structural defects and sulfur impurities in the silicon lattice [9]. They concluded that it most likely came from the sulfur impurity states in silicon. Three impurity centers were found below E_c in silicon by sulfur doping: Type-I (0.18 eV (A) and 0.38 eV (B)), Type-II (0.32 eV (C) and 0.53 eV (D)) and Type-III (0.08 eV). The occurrence of the third center depends on the starting material and diffusion conditions. Both of the concentrations of each defect level

* Corresponding author. Shanghai Ultra-Precision Optical Manufacturing Engineering Center and Department of Optical Science and Engineering, Fudan University, Shanghai 200433, China.
E-mail address: songyouwang@fudan.edu.cn (S.Y. Wang).

http://dx.doi.org/10.1016/j.renene.2014.12.049
0960-1481/

in Type-I are the same and so are Type-II. Moreover, both of Type-I and Type-II are double donors [10]. The IPV effect in silicon solar cell doped with sulfur was studied previously [7]. By numerical simulation, it was found that when $E_c - E_t = 0.18$ eV and $N_t \approx N_a$ for fixed E_t, the PCE was the highest. However, only one defect level was considered in each simulation in Ref. [7]. Moreover, due to the nature of double donors of Type-I and Type-II impurity centers, the three defect levels considered in Ref. [7] will not appear simultaneously in c-Si doped with sulfur. Suppose that there is an infinite number of defects, the limiting efficiency of solar cells with IPV could reach 77.2% under blackbody illumination [11]. Therefore, it is meaningful to investigate whether the efficiency can be improved when more than one defect level is introduced in a c-Si solar cell, doped with sulfur.

2. Model description

In the present work, multiple defect levels are considered. The SCAPS program [12,13] is used to study the n^+–p–p^+ structure of c-Si solar cell doped with sulfur. First, the relations between N_t and PCE with different number of defect levels are studied. Then, all of the defect centers except Type-III are considered and the thickness and background doping concentration of each layer is optimized. The detail of using SCAPS to deal with the IPV effect can be found in Ref. [14].

The SRH recombination model was modified in order to model the IPV effects which include the photo-generation effect through defect level [1,6–8]. As illustrated in Fig. 1(a), an electron is excited from VB to the defect level by a sub-band gap photon, and then another photon is needed to excite the electron to CB. Electrons and holes' transition through the defect levels is governed by capture, thermal and optical emission of carriers.

For a steady-state condition, the net recombination rate U via an impurity level is expressed as [1]:

$$U = \frac{np - (n_1 + \tau_{n0} g_{nt})\left(p_1 + \tau_{p0} g_{pt}\right)}{\tau_{n0}\left(p + p_1 + \tau_{p0} g_{pt}\right) + \tau_{p0}(n + n_1 + \tau_{n0} g_{nt})} \tag{1}$$

where n and p are electron and hole concentrations, respectively, and n_1 and p_1 are electron and hole concentrations after impurity doping when the electron and hole Fermi energy levels E_{Fn}, E_{Fp} coincide with the impurity level E_t which is given by

$$n_1 = N_c e^{-(E_c - E_t)/kT}, \quad p_1 = N_v e^{-(E_t - E_v)/kT} \tag{2}$$

where E_t is the impurity energy level. E_c and E_v are CB and VB edges and N_c and N_v are the effective densities of states in the CB and VB. In Eq. (1) τ_{n0} and τ_{p0} are SRH lifetimes for electron and hole concentrations after illumination while g_{nt} and g_{pt} represent the optical emission rates from the defect for electrons and holes, respectively, which constitute the IPV effect of the modified SRH model. These processes are indicated as E_e^{opt} and H_e^{opt} as it is shown in Fig. 1(a). They are given by

$$\tau_{n0} = \frac{1}{c_n N_t} = \frac{1}{\sigma_n \nu_{th} N_t}, \quad \tau_{p0} = \frac{1}{c_p N_t} = \frac{1}{\sigma_p \nu_{th} N_t} \tag{3}$$

$$g_{nt} = N_t \int_{\lambda_{nmin}}^{\lambda_{nmax}} \sigma_n^{opt}\left(x, \lambda\right) \phi_{ph}\left(x, \lambda\right) d\lambda \tag{4}$$

$$g_{pt} = N_t \int_{\lambda_{nmin}}^{\lambda_{nmax}} \sigma_p^{opt}\left(x, \lambda\right) \phi_{ph}\left(x, \lambda\right) d\lambda \tag{5}$$

where σ_n and σ_p represent the electron and hole capture cross sections, respectively. ν_{th} is the carrier thermal velocity, and N_t is impurity concentration. σ_n^{opt} and σ_p^{opt} are electron and hole photo-emission cross sections of the impurity while $\phi_{ph}(x,\lambda)$ is the photon flux density at depth x from the illuminated surface for wavelength λ. In Eqs. (4) and (5), $\phi_{ph}x$, λ can be expressed as

$$\phi_{ph}(x, \lambda) = \phi_{ext}(\lambda) \frac{1 + R_b e^{-4\alpha_{tot}(\lambda)(L-x)}}{1 - R_b R_f e^{-4\alpha_{tot}(\lambda)L}} e^{-2\alpha_{tot}(\lambda)x} \tag{6}$$

where $\phi_{ext}(\lambda)$ is the external incident photon flux and R_f and R_b represent the internal reflectance at the front and rear surfaces which are used to describe the light trapping effect. $\alpha_{tot}(\lambda)$ is the total absorption coefficient which is given by

$$\alpha_{tot}(\lambda) = \alpha_n(\lambda) + \alpha_p(\lambda) + \alpha_{fc}(\lambda) + \alpha_{eh}(\lambda) \tag{7}$$

where $\alpha_n(\lambda)$ and $\alpha_p(\lambda)$ are the defect absorption coefficients, and $\alpha_{fc}(\lambda)$ is the absorption coefficient of free carriers while $\alpha_{eh}(\lambda)$ represents the band to band absorption coefficient. A detailed approach of this model could be found in Ref. [14].

The n^+-p-p^+ structure as shown in Fig. 1(b) is used in the present calculation with the initial thickness of each layer 0.3 μm, 50 μm and 1 μm, respectively. n^+ is the emitter layer with $N_D = 10^{18}$ cm^{-3} while 10^{17} cm^{-3} and 10^{18} cm^{-3} are the N_a of the p base layer and p^+ layer, respectively. The p^+ layer not only serves as a back surface field (BSF) layer, but also keeps a high value for the built-in-voltage and the impurity level occupied [2]. The p base layer is doped with sulfur.

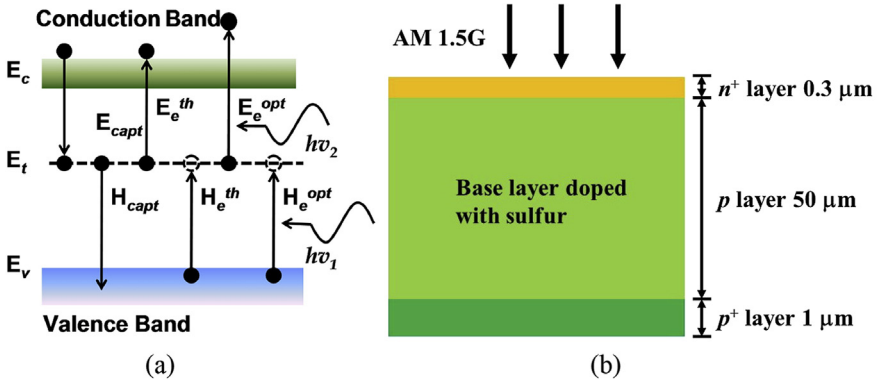

Fig. 1. (a) Illustration of transitions in IPV solar cell. (b) Schematic diagram of the silicon solar cell.

Table 1
The parameters of the impurity centers used in the calculation.

Type of impurity centers	Type-I		Type-II	
Type of defects	Defect A	Defect B	Defect C	Defect D
Energy level (eV)	0.18	0.38	0.32	0.53
σ_n (cm^2) [7,10]	1.5×10^{-14}	2.0×10^{-13}	1.4×10^{-15}	7.0×10^{-14}
σ_p (cm^2) [7]	1.0×10^{-22}	1.0×10^{-22}	1.0×10^{-22}	1.0×10^{-22}

For unpassivated silicon, the surface recombination velocity was as high as 10^7 cm/s [15], however, it can be reduced drastically to as low as 3.0 cm/s with surface passivation method [16]. Here, the recombination velocity at the front and rear surfaces is assumed to be $S_n = S_p = 10^4$ cm/s as used in Ref. [7] though the PCE can be improved further with lower surface recombination velocity [14]. Light trapping condition was very critical to the efficiency improvement of IPV solar cells [14]. $R_f = R_b = 0.99$ was used due to the very little PCE improvement when R_f and R_b was smaller than 0.99. For $R_b = 0.99$, it may be realized by using a Bragg reflector structure while for $R_f = 0.99$, it may be realized with the textured surface [6].

The optical cross sections of the defect levels are calculated by the Lucovsky model [17]. The solar cell parameters were calculated under the standard conditions (AM1.5G, 300 K). The impurity center of Type-III is not considered. The main input parameters used for the c-Si solar cell can be found in Ref. [7]. Parameters used for the impurity centers are listed in Table 1. According to the calculation results [18], for donor-type impurity level, unlike the electron capture cross section (σ_n), the hole capture cross section (σ_p) has a crucial influence on the PCE. Due to no experimental results were found for σ_p in c-Si doped with sulfur, a very little value of $\sigma_p = 1.0 \times 10^{-22}$ cm^2 is used as proposed in Ref. [7] in order to obtain a high PCE. The data of σ_n of defect A, C and D are attained from Ref. [10] while for defect B, it is attained from Ref. [7].

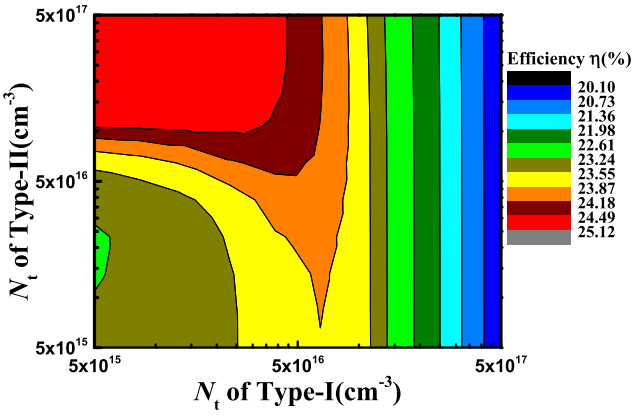

Fig. 3. Influence of N_t of Type-I and II on the efficiency.

3. Numerical results and discussion

First, the simulation was carried out without doping, producing a PCE of 23.22%. Then the influences of concentration of Type-I and II on the performance of IPV solar cells are studied, respectively. Results are shown in Fig. 2. In the simulation, the concentration of each defect level in each impurity center is equal and the sum of them equals N_t. For Type-I, it could be found that the PCE increases with an impurity concentration up to the value of 6.9×10^{16} cm^{-3} and then decreases above this value. The reason for this decrease is that when the impurity concentration nearly equals the background doping concentration, the occupation of the defect state is less than

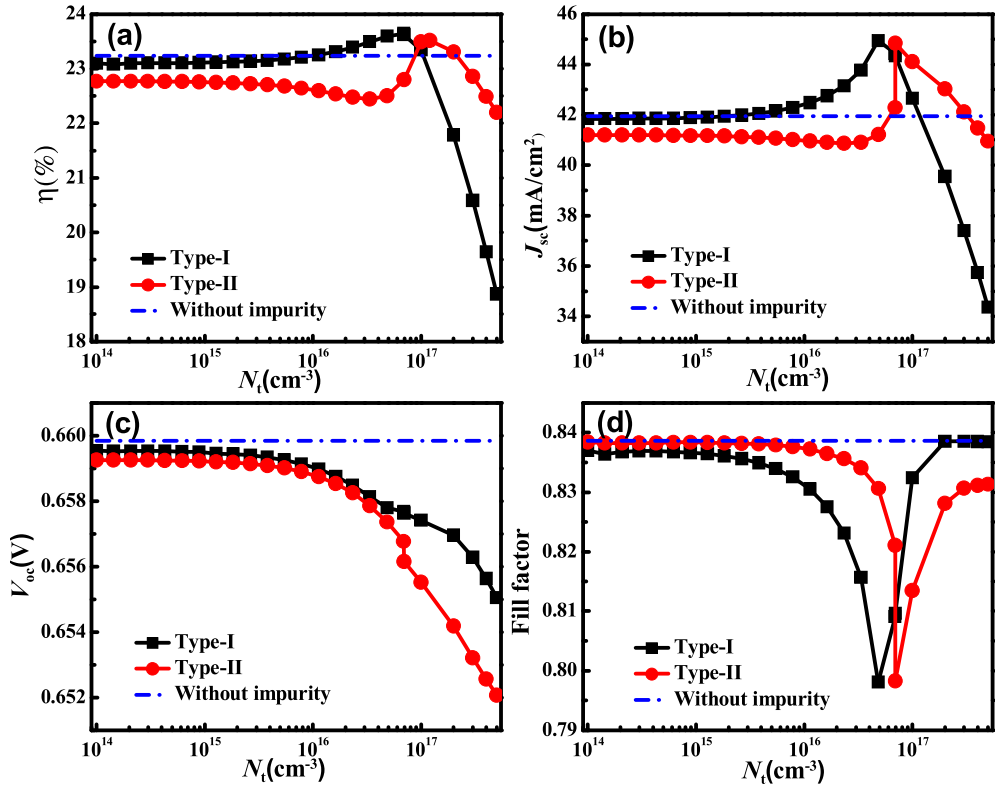

Fig. 2. Dependence of (a) PCE, (b) short circuit current density J_{sc}, (c) open circuit voltage V_{oc} and (d) Fill factor on concentration of sulfur N_t.

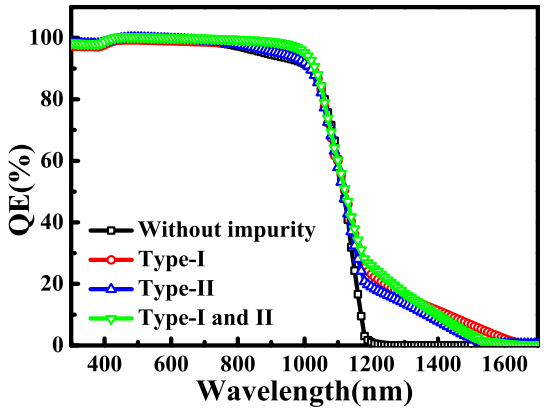

Fig. 4. Quantum efficiency (QE) of different defect levels.

1 which will result in an increase of the transition rate from VB to the defect. Then the transition rate from the defect to CB will be reduced which will reduce the PCE in the end. The same behavior was observed for Type-II except that the highest PCE is attained when $N_t = 1.0 \times 10^{17}$ cm^{-3}. It also can be seen that the variation tendency of PCE with N_t is mainly determined by the variation of J_{sc} with N_t which is shown in Fig. 2(b). The relation between V_{oc} and N_t is shown in Fig. 2(c). It can be found that V_{oc} is lower than that without Type-I or Type-II doping. However, after the doping of sulfur, V_{oc} decreases slowly until the background doping of the p-type base layer is nearly compensated by sulfur because of the heavy doping layer. When N_t is small, for Type-I, J_{sc} is bigger than that without sulfur doping, However, for Type-II J_{sc} is smaller. The reason may be that the impurity levels of Type-II are near the middle of the band gap which will increase the electron–hole recombination through the defects. The same behavior is observed in Ref. [7]. Fig. 2(d) shows the corresponding change in the fill factor with N_t. The decrease in fill factor is due to either an increase in series resistance or a decrease in shunt resistance or both [19].

Then two impurity centers (four defect levels) are all considered and N_t of Type-I and II are optimized together in Fig. 3. Both of the range of Type-I and II are varied from 5×10^{15} to 5×10^{17} cm^{-3}. It can be found that when N_t of Type-I is smaller than 4.5×10^{16} cm^{-3} and Type-II greater than 1×10^{17} cm^{-3}, the efficiency will be the highest. But the SRH model used here can't be used when impurity concentration exceeding 10^{17} cm^{-3} [6]. On the other hand, in order to get a PCE improvement, the impurity concentration should be close to, but not exceed the base doping (10^{17} cm^{-3} in our paper). Therefore, N_t of Type I and Type II are just set to 4×10^{16} cm^{-3} and 6×10^{16} cm^{-3} in the dark red region of the figure in our following simulation.

Fig. 4 gives the QE of different defect levels. For only Type-I being considered, the optimized value of N_t of 6.9×10^{16} cm^{-3} is used while 1×10^{17} cm^{-3} is used for Type-II. In the four defect levels case 4×10^{16} and 6×10^{16} cm^{-3} are used for the N_t of Type I and II, respectively. It can be found that unlike the undoped cell, the infrared response is enhanced with sulfur doping. Moreover, the infrared response wavelength range of the case considering Type-I is wider than that of considering Type-I and II. The main reason may be that too many doping levels enhance the recombination of carriers leading to a deterioration of the solar cell performance. However, the infrared response wavelength range of the case considering Type-II is narrower than that of considering Type-I and II. In order to get the highest PCE, the number and type of defect levels should be controlled at the same time.

Because the thickness of each layer affects the transmission of photo-generated carriers, the influence of thickness of each layer on the PCE of solar cells is investigated. The results are shown in Fig. 5. In Fig. 5(a) it can be found that with the increase of the thickness of n^+, the PCE gradually decreases. The value of 0.3 μm is used for the successive simulation. For the p and p^+ layer, the PCE has a peak at about 80 and 12 μm respectively in Fig. 5(b) and (c). So the thicknesses of 80 μm and 12 μm are used for the p layer and p^+ layer, respectively. It can also be found that the thickness of p^+ has less effect on the PCE than that of n^+ and p layer. In the condition that the structure of our simulation is always n^+–p–p^+, the

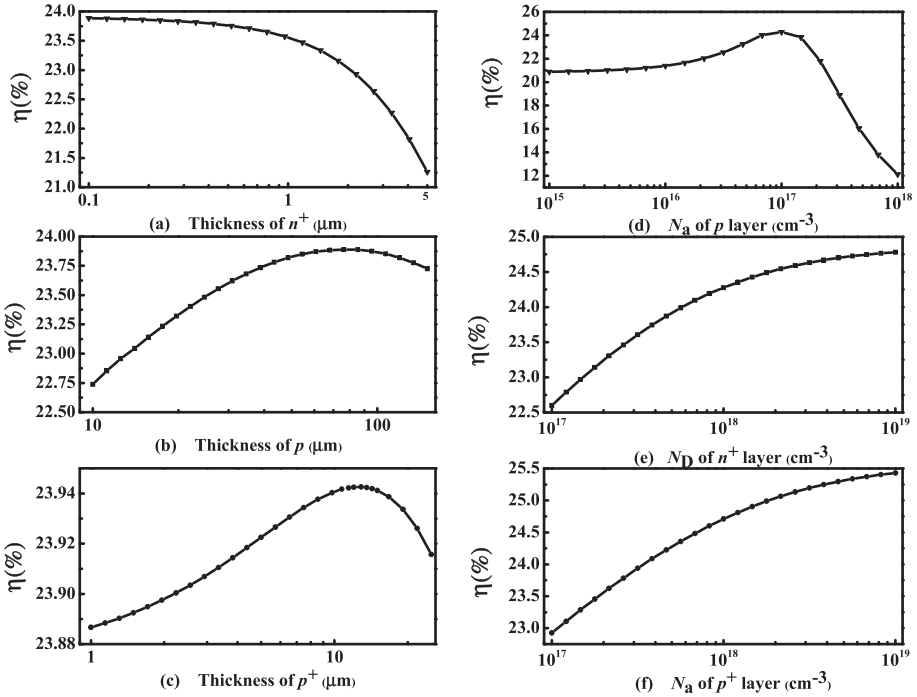

Fig. 5. Influence of the thickness of n^+ (a), p (b), p^+ (c) on the PCE and influence of background doping concentration of p (d), n^+(e), p^+ (f) on the PCE.

relations of background doping concentration of each layer and the PCE are simulated in Fig. 5(d)–(f). The influence of N_a of the p layer on the PCE is given in Fig. 5(d). The PCE increases gradually, reaching a peak at $N_a = 1.0 \times 10^{17}$ cm^{-3}, then rapidly decreases. In Fig. 5(e) and (f), the PCE increase with the N_D of n^+ and N_a of p^+ layer. Both of them are set to 5×10^{18} cm^{-3}. At last the highest PCE of 25.32% is attained in the four defect levels case. It is lower than the highest PCE reported to be 27.45% [7]. The reason may be that when more than one defect is introduced, the recombination process will be enhanced. On the other hand, some of the defect levels are far away from the optimized impurity level [7] which will deteriorate the performance of IPV solar cells. The light trapping condition used by us is less harsh than them as well.

4. Conclusion

In summary, the IPV effect of more than one defect level in a silicon solar cell doped with sulfur is investigated in this paper. By optimizing the thickness and background concentration of each layer, the highest PCE of 25.32% is obtained. This is 2% larger than the value of 23.22% without sulfur doping. The calculation of quantum efficiency showed that the QE are enhanced through doping of sulfur. The infrared response wavelength range of the case considering Type-I is wider than that of considering Type-I and II which showed that it is not always the more defect levels, the better. The infrared response wavelength range of the case considering Type-II is narrower than that of considering Type-I and II, so in order to get the highest PCE, the number and the type of defect levels should be considered. These results are attractive and can provide guidance to the future experimental work of IPV solar cells.

Acknowledgments

The authors thank Dr. Marc Burgelman at University of Gent for software support of SCAPS-1D on request. The work was supported by National Basic Research Program of China (No. 2010CB933703 and 2012CB934303).

References

[1] Keevers MJ, Green MA. Efficiency improvements of silicon solar cells by the impurity photovoltaic effect. J Appl Phys 1994;75:4022.
[2] Schmeits M, Mani AA. Impurity photovoltaic effect in c-Si solar cells. A numerical study. J Appl Phys 1999;85:2207.
[3] Karazhanov SZ. Impurity photovoltaic effect in indium-doped silicon solar cells. J Appl Phys 2001;89:4030.
[4] Beaucarne G, Brown AS, Keevers MJ, Corkish R, Green MA. The impurity photovoltaic (IPV) effect in wide-bandgap semiconductors: an opportunity for very-high-efficiency solar cells? Prog Photovoltaics Res Appl 2002;10:345.
[5] Brown AS, Green MA. Impurity photovoltaic effect with defect relaxation: implications for low band gap semiconductors such as silicon. J Appl Phys 2004;96:2603.
[6] Khelifi S, Burgelman M, Verschraegen J, Belghachi A. Impurity photovoltaic effect in GaAs solar cell with two deep impurity levels. Sol Energy Mater Sol Cells 2008;92:1559.
[7] Azzouzi G, Chegaar M. Impurity photovoltaic effect in silicon solar cell doped with sulphur: a numerical simulation. Phys B 2011;406:1773.
[8] Zhao B, Zhou J, Chen Y. Numerical simulation of the impurity photovoltaic effect in silicon solar cells doped with thallium. Phys B 2010;405:3834.
[9] Wu C, Crouch CH, Zhao L, Carey JE, Younkin R, Levinson JA, et al. Near-unity below-band-gap absorption by microstructured silicon. Appl Phys Lett 2001;78:1850.
[10] Brotherton SD, King MJ, Parker GJ. The electrical properties of sulphur in silicon. J Appl Phys 1981;52:4649.
[11] Brown AS, Green MA. Impurity photovoltaic effect: fundamental energy conversion efficiency limits. J Appl Phys 2002;92:1329.
[12] Burgelman M, Nollet P, Degrave S. Modelling polycrystalline semiconductor solar cells. Thin Solid Films 2000;361–362:527.
[13] Decock K, Khelifi S, Burgelman M. Modelling multivalent defects in thin film solar cells. Thin Solid Films 2011;519:7481.
[14] Khelifi S, Verschraegen J, Burgelman M, Belghachi A. Numerical simulation of the impurity photovoltaic effect in silicon solar cells. Renew Energy 2008;33:293.
[15] Daliento S, Mele L, Bobeico E, Lancellotti L, Morvillo P. Analytical modelling and minority current measurements for the determination of the emitter surface recombination velocity in silicon solar cells. Sol Energy Mater Sol Cells 2007;91:707–13.
[16] Matsumura H, Miyamoto M, Koyama K, Ohdaira K. Drastic reduction in surface recombination velocity of crystalline silicon by surface treatment using catalytically-generated radicals. Sol Energy Mater Sol Cells 2011;95:797–9.
[17] Lucovsky G. On the photoionization of deep impurity centers in semiconductor. Solid State Commun 1965;3:299.
[18] Yuan J, Shen H, Huang H, Deng X. Positive or negative gain: role of thermal capture cross sections in impurity photovoltaic effect. J Appl Phys 2011;110:104508.
[19] Sahoo HS, Yadav AK, Ray A. Simulation of IPV effect in in-doped c-Si with optimized indium concentration and layer thickness. Phys B 2011;406:4221–6.